Supplementary Tables

Table S1: Compositions of synthesized compounds, as indicated by atomic ratios measured by ICP.

Compound	Target ratio Li : Mn : V : F	Measured ratio Li : Mn : V : F
ST-LMVO	1.143 : 0.286 : 0.572 : 0	1.155 : 0.268 : 0.571 : 0
ST-LMVF20	1.171 : 0.343 : 0.486 : 0.2	1.180 : 0.329 : 0.461 : 0.213
MR-LMVF20	1.133 : 0.400 : 0.467 : 0.2	1.141 : 0.405 : 0.474 : 0.204
LR-LMVF20	1.230 : 0.255 : 0.515 : 0.2	1.236 : 0.252 : 0.518 : 0.201
LR-LMVO	1.200 : 0.200 : 0.600 : 0	1.211 : 0.198 : 0.590 : 0

Supplementary Figures

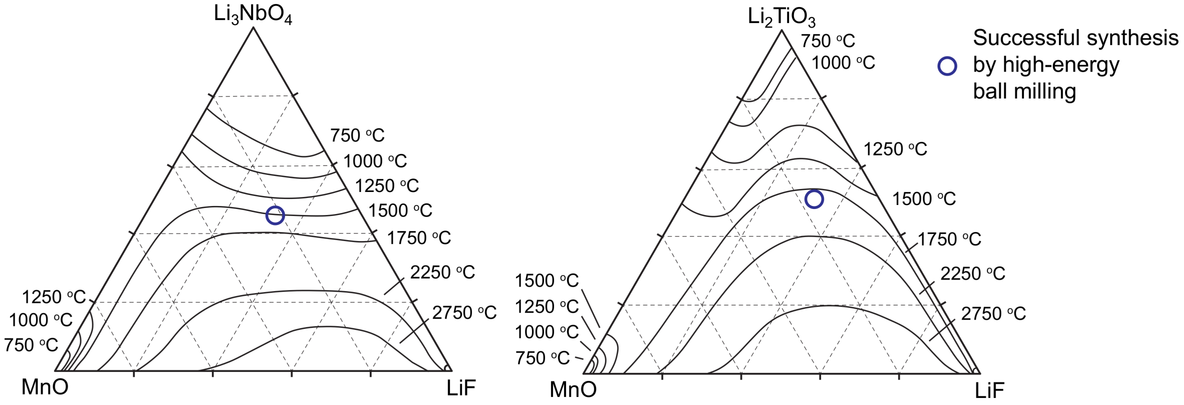

Figure S1: Computed phase diagram of the MnO-Li_3NbO_4-LiF and MnO-Li_2TiO_3-LiF systems, marking the previously reported compositions successfully synthesized by high–energy ball-milling. As the reported compositions are stabilized at approximately 1750 °C, we choose stability at 1750 °C as a heuristic for synthetic accessibility by high–energy ball–milling.

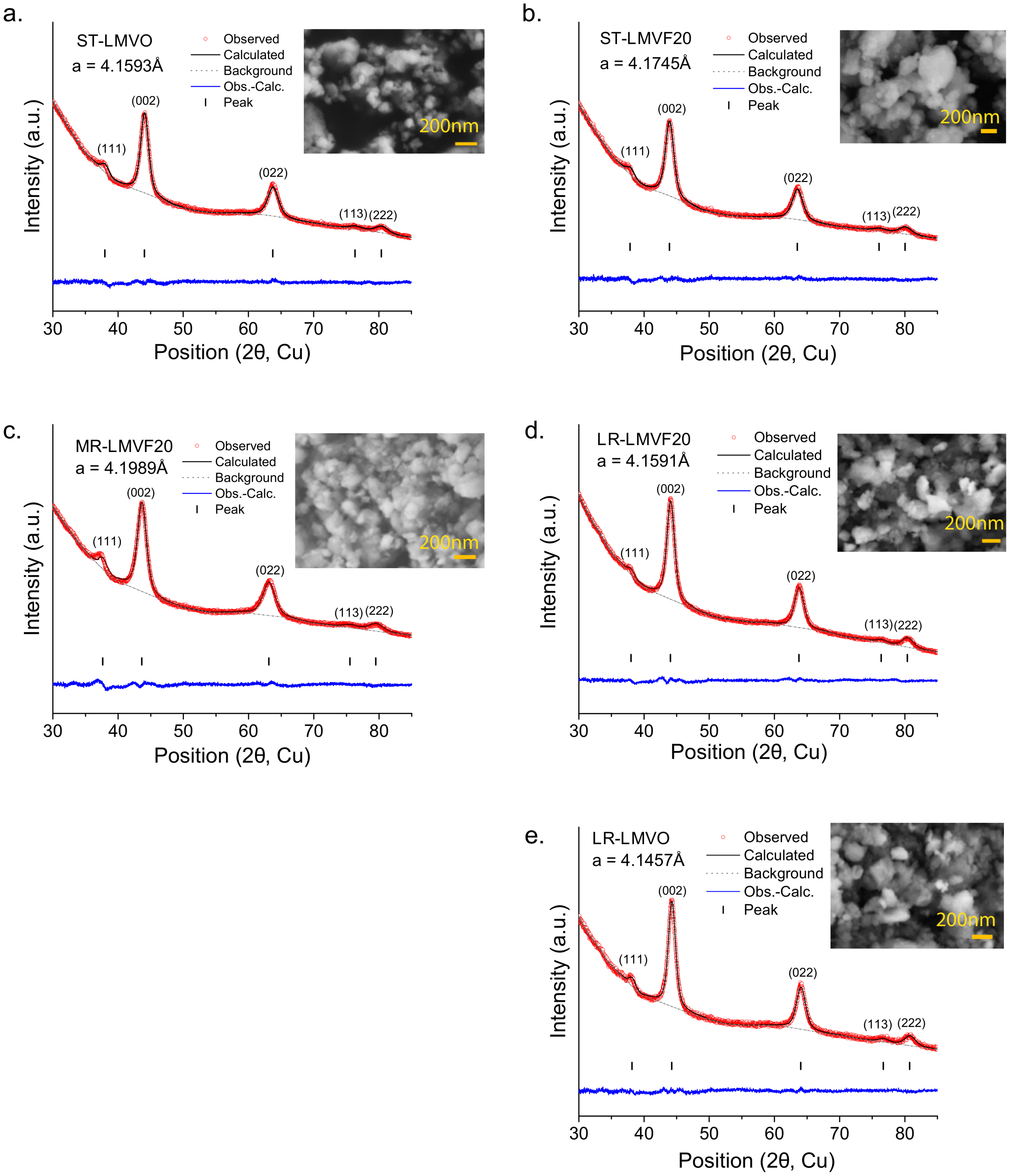

Figure S2: XRD refinement and scanning electron microscopy (SEM) imaging of the secondary particles of **a.** ST-LMVO, **b.** ST-LMVF20, **c.** MR-LMVF20, **d.** LR-LMVF20, **e.** LR-LMVO.

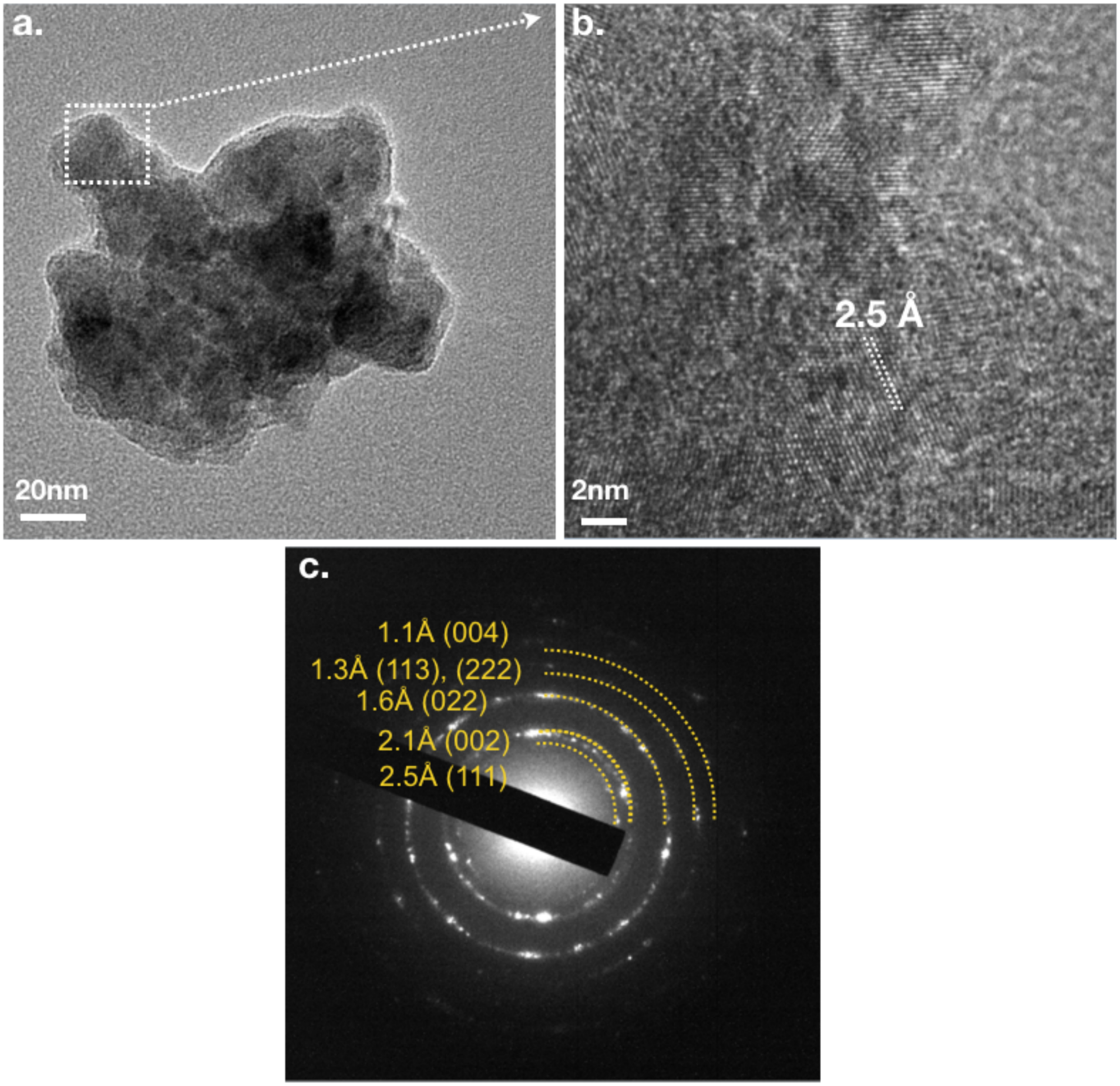

Figure S3: **a.** TEM and **b.** HRTEM image and **c.** electron diffraction pattern of ST-LMVF20. The TEM image shows that the secondary particle size of the ST-LMVF20 is around 100 nm. The HRTEM image is taken within the dashed-line square area in **a.**, and we can see different oriented fringes, which indicates the particle is polycrystalline. The electron diffraction pattern shows the characteristic diffraction rings of a disordered rock-salt structure, which further proves that the as-synthesized material is a polycrystalline disordered rock-salt.

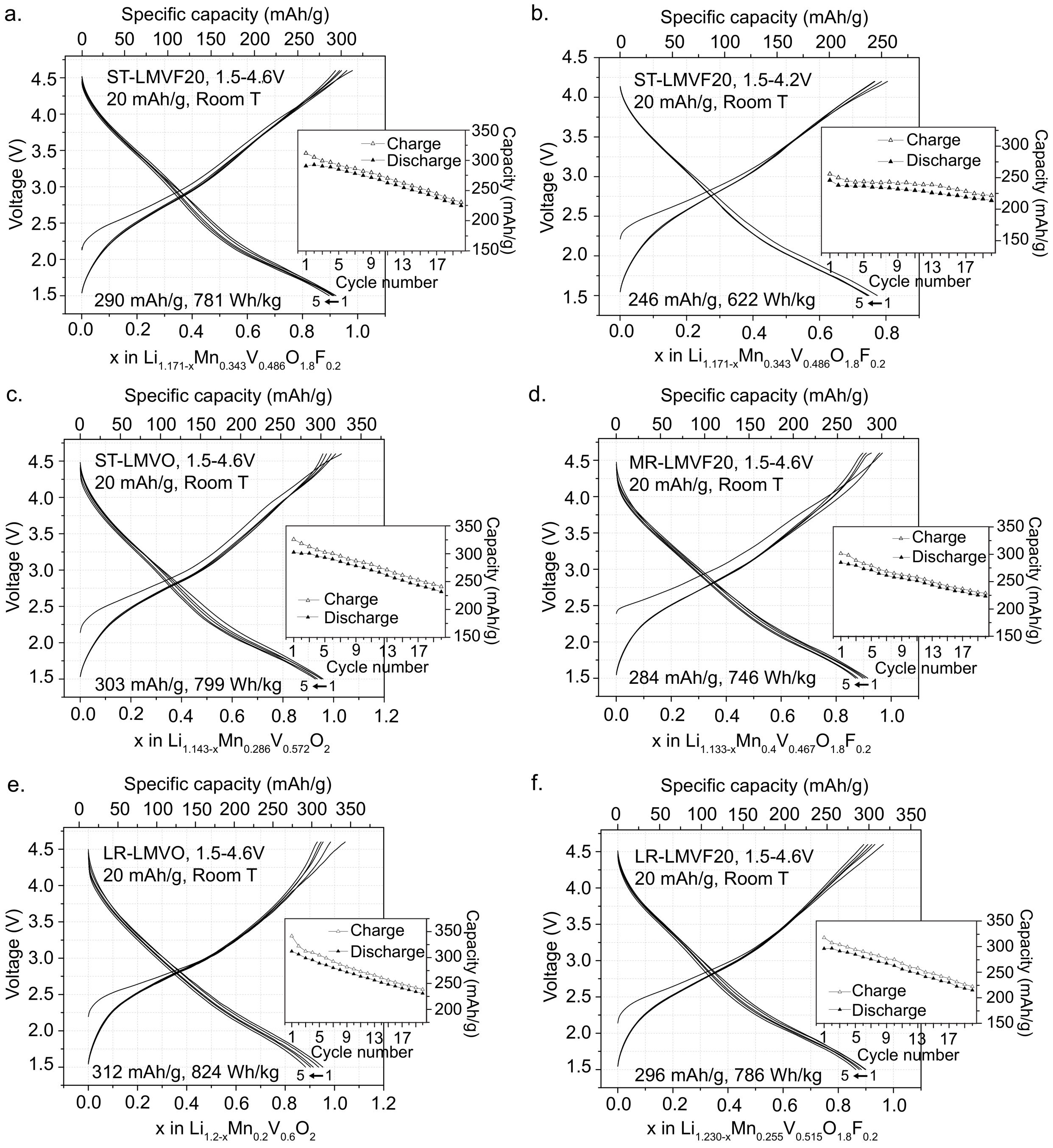

Figure S4: Galvanostatic voltage profiles for charge–discharge cycles, and associated capacity retention in **a.,b.**, ST-LMVF20 (4.6V, 4.2V cutoff), **c.** ST-LMVO (4.6V), **d.** MR-LMVF20 (4.6V), **e.** LR-LMVF20 (4.6V) and **f.** LR-LMVO (4.6V).

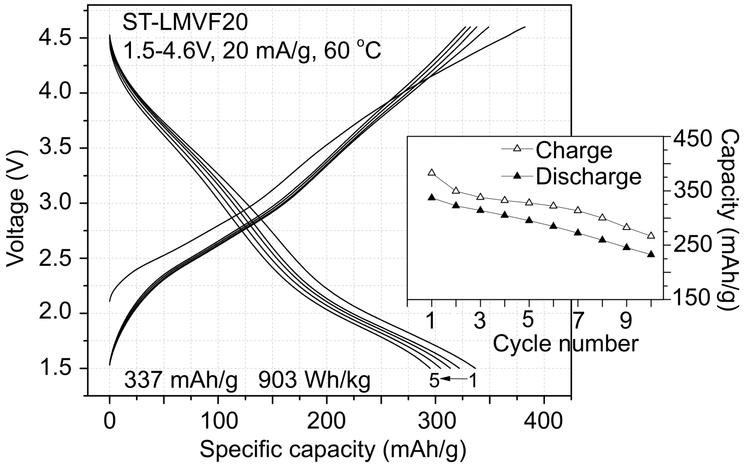

Figure S5: High temperature galvanocycle cycling profile of ST-LMVF20.

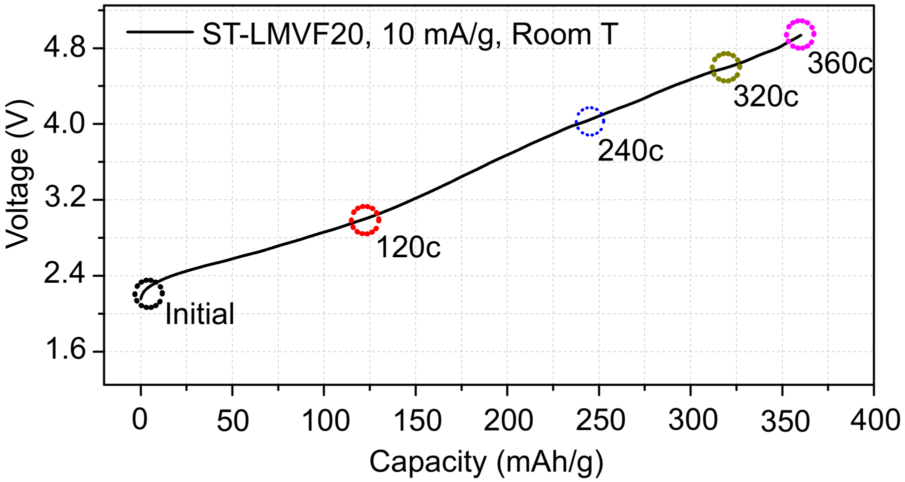

Figure S6: Voltage profile of first-charge samples used for XAS characterization.

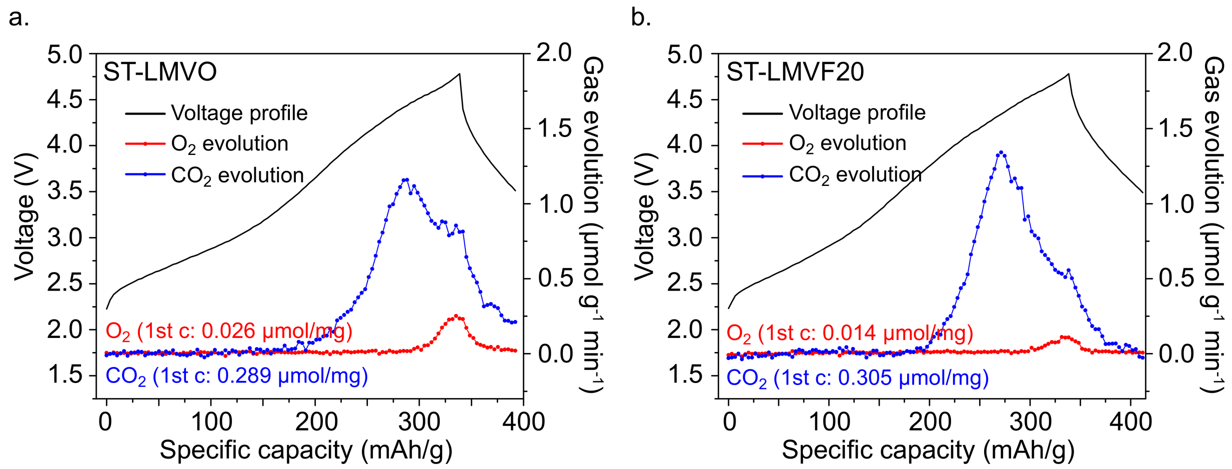

Figure S7: First-cycle DEMS for 7:2:1 cathode film (active material:carbon black:PTFE) for (**a.**) ST-LMVO and (**b.**) ST-LMVF20, illustrating the characteristic decrease in oxygen evolution upon fluorination. We attribute the large CO_2 evolution peak in both materials to the first–cycle decomposition of carbonates at the surface, while the O_2 evolution profile is representative of the relative amount of oxygen loss from the active material.

The DEMS results shown in in Figure S7 reveal a noticeable amount of CO_2 gas evolution, which can be mainly attributed to the decomposition of surface carbonate as reported previously.[S1,S2] However, this contribution to the overall capacity is small. Renfrew *et al.*[S2] point out that surface Li_2CO_3 oxidation does contribute to the first cycle capacity, but DEMS results by W. H. Kan *et. al.*[S3] show that CO_2 evolution is greatly reduced in the second charge, indicating that Li_2CO_3 oxidation is for the most part irreversible. In our materials, while there is clearly some Li_2CO_3 oxidation, its contribution to the overall capacity must be small as we measure highly reversible performance over repeated charge/discharge cycles. The voltage profile of ST-LMVF20 shown in Fig. 3a is mostly unchanged over the first five cycles, with almost no capacity fade and a Coulombic efficiency in excess of 94% even for the first cycle. These findings indicate that any surface Li_2CO_3 oxidation is small compared to bulk transition metal oxidation as otherwise we would observe much more obvious capacity fade and smaller Coulombic efficiency.

References

[S1] Lee, J.; Kitchaev, D. A.; Kwon, D.-H.; Lee, C.-W.; Papp, J. K.; Liu, Y.-S.; Lun, Z.; Clément, R. J.; Shi, T.; McCloskey, B. D.; Guo, J.; Balasubramanian, M.; Ceder, G. *Nature* **2018**, *556*, 185.

[S2] Renfrew, S. E.; McCloskey, B. D. *J. Am. Chem. Soc.* **2017**, *139*, 17853–17860.

[S3] Kan, W. H.; Chen, D.; Papp, J. K.; Shukla, A. K.; Huq, A.; Brown, C. M.; McCloskey, B. D.; Chen, G. *Chem. Mater.* **2018**, *30*, 1655–1666.